Cerebral Cortex March 2008;18:508–515
doi:10.1093/cercor/bhm090
Advance Access publication June 18, 2007

Lateralized Anterior Cingulate Function during Error Processing and Conflict Monitoring as Revealed by High-Resolution fMRI

Henry Lütcke and Jens Frahm

Biomedizinische NMR Forschungs GmbH am Max-Planck-Institut für biophysikalische Chemie, 37070 Göttingen, Germany

Recent studies have reported that functional subdivisions of anterior cingulate cortex (ACC) may be selectively responsible for conflict and error-related processing. We examined this claim by imaging ACC activation to correct and erroneous response inhibitions in a GoNogo task. After localizing the ACC cluster in individual subjects using functional magnetic resonance imaging (fMRI) at standard resolution ($2 \times 2 \times 4$ mm^3), high-resolution fMRI ($1.5 \times 1.5 \times 1.5$ mm^3) of the ACC was performed in a second session to investigate its precise functional anatomy. At standard resolution, and in agreement with previous studies, ACC was activated for correct and incorrect responses, albeit more so for errors. High-resolution maps of activated ACC clusters revealed localized and reproducible foci in 9 out of 10 volunteers. Multisubject analysis suggested a bilateral distribution of error-related processes in ACC, whereas correct inhibitions only seemed to activate ACC in the right hemisphere. Subsequent region of interest analysis largely confirmed the activation maps. Our results contribute toward a better understanding of the microanatomy of ACC and demonstrate the potential of fMRI for mapping the functional architecture of brain regions involved in cognitive tasks at a previously unaccomplished spatial scale.

Keywords: ACC, fMRI, high resolution, lateralization

Introduction

In a permanently changing environment, only few things seem to be more important for the pursuit of stable, long-term goals than the ability to constantly monitor one's own actions, initiate changes in the face of new external demands, or abandon unsuccessful strategies altogether. Such a capacity for cognitive control may well be one of the hallmarks of human behavior.

Numerous studies have identified the medial frontal cortex (MFC), and especially its anterior cingulate part (ACC), as one of the most reliable neural correlates of cognitive control in the human brain (Carter et al. 1998; Botvinick et al. 1999, 2004; Ridderinkhof, Ullsperger, et al. 2004; Ridderinkhof, van den Wildenberg, et al. 2004; Ullsperger and von Cramon 2004). Nevertheless, the precise mechanisms underlying this function are still a matter of debate. Whereas initial EEG experiments suggested that ACC might play a role in the detection of errors (Falkenstein et al. 1991; Gehring et al. 1993), subsequent functional magnetic resonance imaging (fMRI) studies argued for a more global role in monitoring of conflicting action sequences (Carter et al. 1998; Kiehl et al. 2000; Menon et al. 2001). Error detection, in this framework, is thought to occur once conflict rises above a certain threshold (Yeung et al. 2004).

More recently, a functional subdivision of ACC has been proposed (Polli et al. 2005; Taylor et al. 2006). Based on fMRI evidence, Taylor et al. (2006) suggested that the dorsal part of ACC plays a role in conflict monitoring, whereas its rostral component may be more involved in error-specific processing such as performance evaluation. Furthermore, these authors demonstrated a surprising degree of intersubject variability for activation foci along the mesial wall, suggesting that discrepancies in the localization of conflict or error-related processing between previous studies may be due to differential clustering of the subjects' activation in the different samples. Moreover, because the spatial resolution of respective experiments has been limited, important differences at an even finer scale may have been missed. In fact, most standard fMRI studies employ voxel sizes in the order of $3 \times 3 \times 3$ mm^3, whereas the technique itself allows for acquisitions with at least an 8 times smaller voxel size of $1.5 \times 1.5 \times 1.5$ mm^3.

Here, we used high-resolution fMRI in combination with a conflict eliciting GoNogo task to investigate the functional anatomy of the ACC at a previously unaccomplished spatial scale. The task, which was designed to generate high proportions of errors on Nogo trials, allowed us to compare putative neural correlates of conflict as well as of error-monitoring processes. Whereas successful conflict resolution implicates only conflict monitoring, error trials involve both conflict and error-related mechanisms.

fMRI at high spatial resolution has previously been used to study early sensory processes, mainly in the visual system, (Schneider et al. 2004; Schwarzlose et al. 2005; Grill-Spector et al. 2006). These studies benefited from the good functional contrast-to-noise ratio (CNR) as well as limited intersubject variability in sensory areas. Cognitive neuroimaging, on the other hand, suffers from low CNR and high variability, making it apparently unsuitable for high-resolution fMRI. Thus, a more general aim of the current study was to investigate the feasibility of a new strategy for cognitive neuroimaging combining low and high spatial resolution.

Materials and Methods

Subjects

Eleven right-handed volunteers (3 males and 8 females; mean age 27 ± 6 years) participated in 2 experimental sessions (separated by more than 1 day). One data set was excluded due to excessive motion (relative displacement in any direction of more than 1 mm). In each experimental session, subjects performed between 4 and 6 repetitions of the experiment, leaving us with a total of 50 standard and 64 high-resolution runs for analysis. Given the substantial variability in activation between subsequent runs, partly attributable to factors such as fatigue, motivation, or hardware changes, each experiment was treated independently for the purpose of statistical analysis. To investigate reproducibility of high-resolution activation maps, one male subject took part in 2 high-resolution sessions (separated by 6 months). All participants were informed about the purpose of the study as well as possible risks

associated with magnetic resonance imaging (MRI). Written consent was obtained prior to each experimental session. After the end of the second session, subjects were debriefed about the staircase procedure (see below). Participants earned 10 Euros per hour plus a bonus depending on their performance (see below). All experimental procedures conformed fully to institutional guidelines.

Task

We used a visual letter-based GoNogo task where subjects had to press a button with their right thumb or index finger whenever a Go (target) stimulus (A, J, S, O) appeared in the center of the screen. Subjects were instructed to refrain from pressing the button upon presentation of a Nogo (nontarget) stimulus (X).

All stimuli were presented in black color on a gray background. Two yellow vertical bars were continuously presented above and below the stimulus location, in order to direct subjects' attention to the center of the screen and to provide feedback (see below).

A total of 120 stimuli were presented per run (20% Nogo) with jittered stimulus onset asynchrony (2, 4, 6 s; mean 4 s) using a dedicated projection setup (Schäfter & Kirchhoff, Hamburg, Germany) or MRI-compatible liquid crystal display goggles (Resonance Technology Inc., Northridge, CA). Corrective lenses were applied if necessary.

The initial presentation duration for all stimuli was 500 ms, and subjects were instructed to respond within this time frame. Subjects were informed about an error (late response to target or response to nontarget) immediately after a trial by briefly changing the color of the vertical bars to red. Usually subjects achieve high performance accuracy on this task (less than 10% false alarms [FAs]), which makes the analysis of errors virtually impossible. Therefore, we modified the presentation time of targets over the course of each run depending on subjects performance on Nogo trials. More precisely, 2 consecutive successful inhibitions led to a reduction of the Go stimulus duration by 50 ms (minimum presentation time 250 ms), whereas 2 consecutive responses to Nogo stimuli increased target duration by 50 ms (maximum presentation time 750 ms). These values were found to yield approximately 50% errors during pretesting. Importantly, the presentation duration of Nogo stimuli was always 500 ms. Participants received a small bonus for correct trials, whereas errors incurred a financial penalty.

Magnetic Resonance Imaging

All studies were conducted at 2.9 T (Siemens Tim Trio, Erlangen, Germany) using a 12-channel receive-only head coil. Each session comprised T_1-weighted MRI (3D FLASH) at $1 \times 1 \times 1$ mm^3 resolution for anatomic referencing. For fMRI, we employed a single-shot gradient-echo echo planar imaging sequence (repetition time/echo time = 2000/36 ms, flip angle 70°, 244 volumes per run). Scans with a voxel size of $2 \times 2 \times 4$ mm^3 were based on a 84×96 acquisition matrix (192 mm field of view [FOV], 7/8 partial Fourier phase encoding, bandwidth 1336 Hz/pixel, echo spacing 0.81 ms) and comprised 22 transverse-to-coronal slices, covering the whole cerebrum. High-resolution fMRI with a voxel size of $1.5 \times 1.5 \times 1.5$ mm^3 was achieved using a 90×128 matrix (180×192 mm rectangular FOV, 6/8 partial Fourier phase encoding, bandwidth 1396 Hz/pixel, echo spacing 0.86 ms) with 18 slices, positioned so as to achieve good coverage of the previously determined active region in ACC. All magnetic resonance images are presented in accordance with radiological convention throughout the manuscript (i.e., right and left sides are flipped).

Data Analysis

Evaluation of fMRI data was performed using tools from the FMRIB Software library (FSL, www.fmrib.ox.ac.uk) and MATLAB (The MathWorks, Natick, MA). After initial motion correction in *k*-space (Siemens), residual motion was accounted for by image-based registration (Jenkinson et al. 2002). Data at standard resolution were smoothed using a Gaussian kernel of full width half maximum (FWHM) 5 mm. Non-brain tissue was removed (Smith 2002), and all volumes were intensity normalized by the same factor and temporally high-pass filtered (Gaussian-weighted least-squares straight line fitting, with high-pass filter cutoff at 30 s). High-resolution data were preprocessed in a similar way, but, instead of Gaussian smoothing, the images were filtered with the smallest univalue segment assimilating nucleus noise reduction algorithm, also part of FSL (Smith and Brady 1997). Intensity thresholds for the definition of anatomical regions were set to one tenth of the maximum image intensity, separately for each volume, and smoothing was performed within regions of similar intensity using a 5-mm Gaussian kernel.

To compare brain responses associated with correctly resolved and erroneous Nogo trials, we created models for correct rejections (CRs) and FAs by convolving relevant events with a Gamma function that takes into account temporal properties of the hemodynamic response to neural activation. Model fit was determined by statistical time series analysis with local autocorrelation correction (Woolrich et al. 2001).

Standard resolution images were spatially normalized to the Montreal Neurological Institute 152 (MNI152) template brain, and mixed-effects group analysis was performed (Beckmann et al. 2003; Woolrich et al. 2004). Significant activations based on z statistic (Gaussianized T/F) images were obtained by first determining clusters of $z > 3.1$ and then applying a corrected cluster threshold of $P = 0.05$, as previously described (Worsley et al. 1992).

High-resolution images were spatially normalized to their respective anatomic scan as well as to the MNI152 template brain (Jenkinson and Smith 2001; Jenkinson et al. 2002) and summarized for each subject (fixed effects). Statistical inference was restricted to an anatomically defined region of interest (ROI) covering the entire MFC. We considered voxels active that surpassed an uncorrected threshold of $P < 0.01$ and had at least 5 activated neighbors. This rather liberal thresholding was motivated by the less severe multiple comparison problem due to spatial restrictions on statistical inference as well as the fact that maps of individual subjects were analyzed. A second higher level analysis examined effects across all subjects and over the whole volume covered. Thresholded activation maps were obtained by controlling the false discovery rate (FDR), which does not rely on spatial smoothness, at $q < 0.01$ (Genovese et al. 2002).

Subsequently, ROIs in dorsal ACC (dACC) and rostral ACC (rACC) were defined individually for each subject by drawing a line at the anterior boundary of the genu of the corpus callosum that was at right angles to the intercommisural plane (Devinsky et al. 1995; Polli et al. 2005). Rostral and dorsal parts were further subdivided according to hemisphere, yielding 4 ROIs. Normalized mean parameter estimates (beta values) from these regions as well as the number of activated voxels in each ROI were subjected to statistical analysis (all P values Bonferroni corrected for multiple comparisons).

Results

Psychophysics

There were no significant differences for any of the behavioral measures (reaction time and accuracy) between the standard and high-resolution sessions (see Table 1). The error rate on Nogo trials was high (57 ± 7% CRs), demonstrating validity of the staircase procedure.

Neuroimaging: Standard Resolution

Linear contrasts between CR and FA were calculated from their model parameter estimates. As expected, contrasting FA and CR (FA > CR) revealed a significant ($z > 3.1$ and corrected cluster $P < 0.05$) activation cluster in MFC as shown in Figure 1 (see

Table 1

Reaction time (RT) and accuracy (±standard deviation) during standard and high-resolution fMRI (sessions 1 and 2, respectively)

	Session 1	Session 2
	Standard resolution	High resolution
Target response (%)	86 ± 11	89 ± 10
Nontarget inhibition (%)	57 ± 7	57 ± 7
RT target response (ms)	360 ± 20	351 ± 19
RT FA (ms)	343 ± 23	333 ± 22

also Table 2). To explore the individual variability of this group activation cluster, we summarized individual runs for each subject and projected the center of gravity (COG) of the largest cluster in MFC into standard space. Although subjects' activation scattered around the cluster obtained from group analysis, there was also a considerable degree of variability, most notably along the dorsal–rostral axis of the MFC. In addition, error-related brain responses were detected in insular, extrastriate and motor cortices bilaterally, right postcentral gyrus, thalamus, as well as midbrain (see Table 2). Specific activation due to successful resolution of conflict (as measured by contrasting CR > FA, Fig. 1) was detected in a cluster in right inferior parietal lobule as well as right orbitofrontal cortex (see Table 2). No MFC activation was observed for this contrast.

Neuroimaging: High Resolution

To examine shared and distinct regions of error and conflict processing in MFC, we calculated linear contrasts between FA and rest (FA > Rest) as well as CR and rest (CR > Rest), respectively. Significant error-related brain responses at the preset criteria ($P < 0.01$, 5 connected voxels) were detected in 9/10 subjects. Activation maps of 2 representative volunteers, displayed on their respective anatomic scans, are shown in Figure 2. Although there appears to be "less activation" compared with conventional acquisitions at lower resolution, all significant voxels are located in the cortical gray matter and respect sulcal architecture. Interestingly, activation in response to impulse errors appears to be more pronounced in the ACC of the right hemisphere, although small foci are also present in left ACC. Note also that active clusters scatter along the whole length of ACC, even for single volunteers. To assess reliability of these maps, the high-resolution session was repeated in one subject. Individual foci colocalized to a surprising degree for these 2 sessions as demonstrated in Figure 3. Taken together, these findings suggest that the ACC foci obtained by high-resolution fMRI represent actual centers of neural activity that are blurred across anatomical borders by standard fMRI acquisition and analysis.

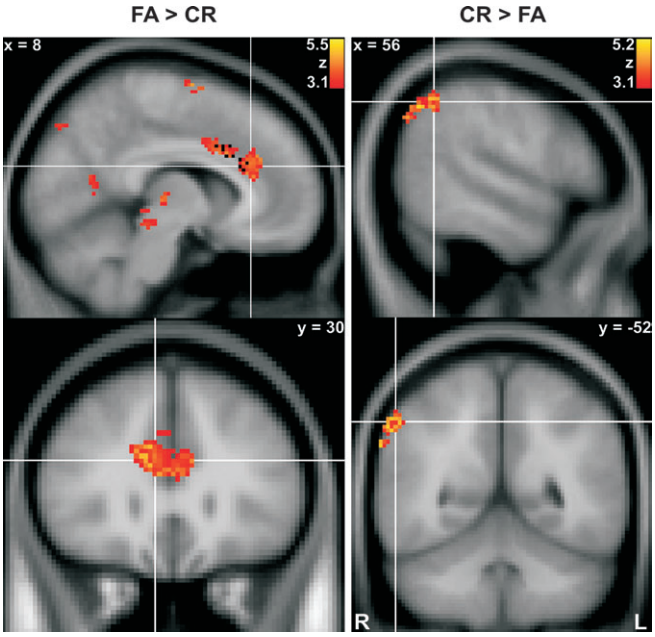

Figure 1. Low-resolution activation maps (averaged across 10 subjects) for responses to FAs and CRs. (Left) Contrasting FA with CR revealed significantly activated clusters ($z > 3.1$; $P < 0.05$) in ACC, thalamus, midbrain, and extrastriate visual areas. Black dots indicate the COGs of individual MFC activation clusters for 7 subjects (projected onto $x = 8$). (Right) The contrast between CR and FA revealed an activated cluster in right inferior parietal cortex.

Table 2

Atlas coordinates (in MNI space) and maximum *z* scores for the COGs of clusters significantly activated in contrasts between FAs and CRs at standard resolution

Contrast	Brain region	COG coordinates (*x*, *y*, *z*)	*z* Score
FA > CR	MFC	3, 19, 33	5.32
	Left insular cortex	−40, −4, −2	5.48
	Right insular cortex/postcentral gyrus	54, −17, 24	4.89
	Left/right extrastriate cortex	±34, −79, 22	5.23
	Right motor cortex	35, −34, 60	4.22
	Left motor cortex	−26, −41, 68	4.90
	Thalamus	−2, −24, 0	5.37
	Midbrain	6, −30, −12	4.22
CR > FA	Right inferior parietal lobule	53, −62, 43	4.96
	Right orbitofrontal cortex	42, 44, −20	5.16

Whereas ACC responded very strongly to FA, we could also detect a weak but significant activation for successful inhibitions in 8/10 subjects (as assessed by CR > Rest; see Fig. 2). CR foci were exclusively localized in the right ACC and largely overlapped with error-responsive activation clusters.

Results obtained from the evaluation of individual volunteers were confirmed and extended by a multisubject analysis. Significant ($q < 0.01$, FDR) and overlapping brain responses to FA > Rest and CR > Rest were detected in MFC (see Fig. 4). The error-related activation cluster was predominantly localized in the right ACC although activation was also seen in the left hemisphere (COG at $x = 2$, $y = 17$, $z = 34$; $z_{max} = 5.1$). In agreement with single subject results, activation for successful inhibitions was exclusively right lateralized (COG: 5, 21, 34; $z_{max} = 3.8$). Apart from activation in MFC, this analysis revealed a region in the right frontopolar cortex that responded significantly to both CR > Rest (COG: 36, 48, 20; $z_{max} = 4.6$) and FA > Rest (COG: 37, 43, 23; $z_{max} = 4.4$; see Fig. 4).

To exclude the possibility that error and conflict-related activations in MFC and prefrontal cortex are unspecific effects of stimulus presentation, we analyzed brain responses to correctly resolved target responses (compared with rest). As expected, an active cluster in left motor cortex (COG: –46, –17, 53; $z_{max} = 6.4$) could be detected in this case (data not shown). Furthermore, erroneous button presses on Nogo trials also elicited activation in left motor cortex (COG: –47, –14, 50; $z_{max} = 5.3$), whereas successful inhibitions failed to do so (data not shown).

A direct comparison of standard and high-resolution activation maps is impeded by the latter's low signal-to-noise ratio (SNR). To nevertheless illustrate the correspondence between standard and high-resolution fMRI, we calculated group activation maps for the FA > CR contrast (Supplementary Fig. 1) for both acquisitions. To account for the SNR difference, the standard resolution maps were required to pass a more stringent threshold ($q < 0.01$ vs. $q < 0.1$, FDR). An overlapping activation cluster in ACC was detected with standard and high-resolution acquisition, demonstrating the correspondence between the 2 approaches (Supplementary Fig. 1).

To quantify the high-resolution fMRI results, we determined the number of active voxels in response to FA, CR, and correct target responses for each experiment separately (thresholded at

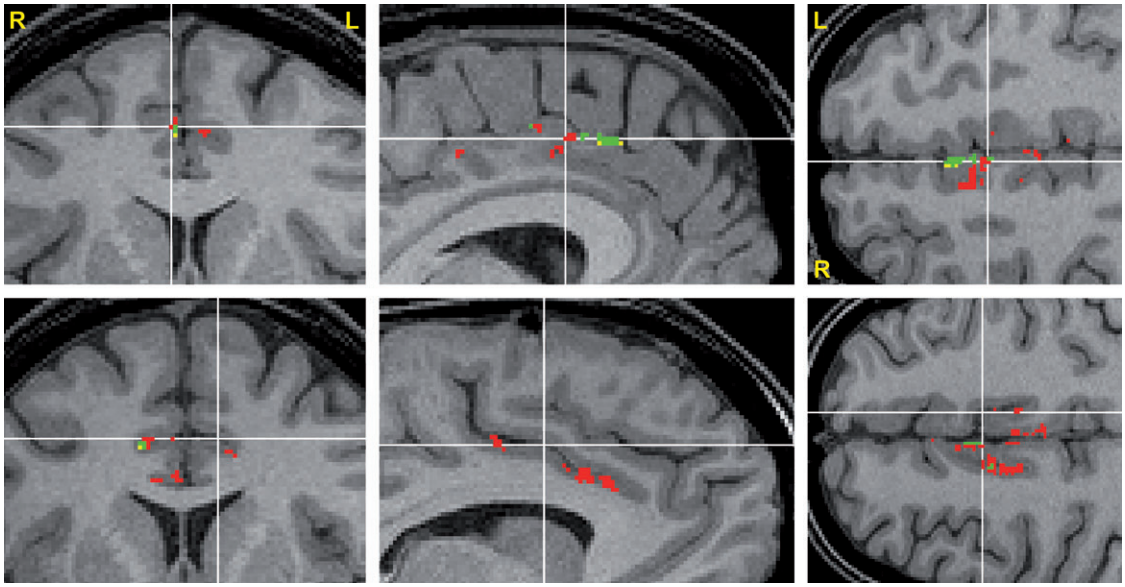

Figure 2. High-resolution activation maps (single subjects) for responses to FAs (FA > Rest) and CRs (CR > Rest). Maps were obtained by averaging across runs and projecting the results on the subjects' individual anatomy. Although active clusters scatter along the length of ACC, they are located in the cortical gray matter and respect sulcal architecture. Top and bottom rows show representative maps from 2 volunteers that demonstrate that active FA > Rest clusters (red) are located mainly, but not exclusively, in the right ACC. Significant responses to CR > Rest (yellow) occurred only in right ACC and overlapped (green) substantially with FA > Rest clusters.

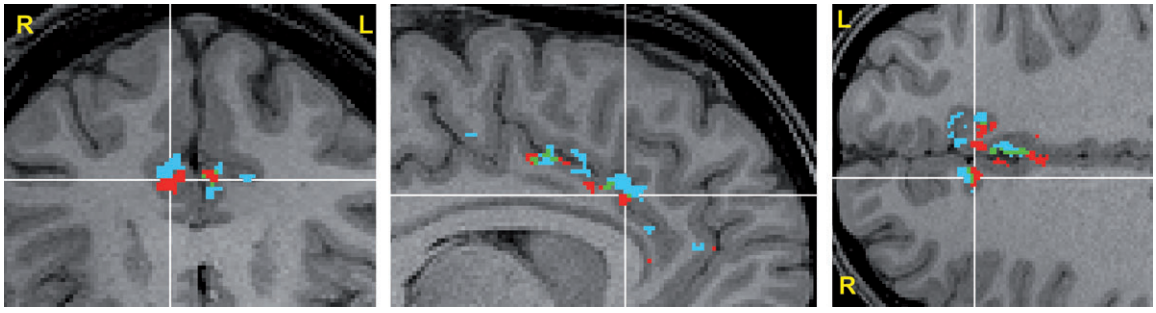

Figure 3. Activation maps for the contrast FA > Rest of a single subject obtained 6 months apart (time point 1: red; time point 2: blue) show a surprising colocalization as well as substantial overlap (green).

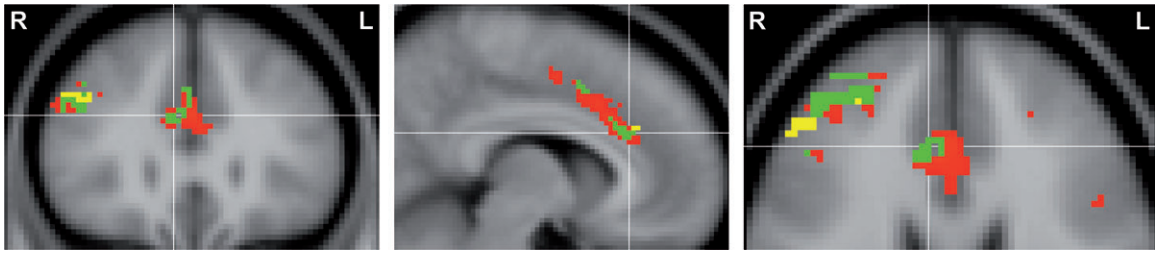

Figure 4. High-resolution activation maps (averaged across 10 subjects) for responses to FAs (FA > Rest, red) and CRs (CR > Rest, yellow). Largely bilateral activation of ACC was associated with impulse errors, whereas successful inhibitions only activated a smaller area in right ACC that overlapped (green) with the corresponding FA cluster. Further, partly overlapping, FA and CR activation was detected in the right frontopolar cortex (coronal and horizontal sections).

$P < 0.01$, 5 connected voxels) in 4 subregions of ACC (see Materials and Methods). A 2 × 3 (hemisphere: left – right; trial type: correct target response – CR – FA) analysis of variance (ANOVA) was carried out separately for dACC and rACC (see Fig. 5). Significant main effects for hemisphere and trial type were obtained in both dACC ($F_{1,63} = 5.6$, $P < 0.05$; $F_{1,78} = 19.7$, $P < 0.001$, respectively) and rACC ($F_{1,63} = 6.7$, $P < 0.05$; $F_{1,82} = 10.5$, $P < 0.01$, respectively). A significant interaction between both factors, indicating a differential modulation of the 2 hemispheres by CR and FA, was evident in rACC ($F_{2,114} = 3.6$, $P < 0.05$) but not dACC ($F_{2,107} = 0.2$, $P > 0.1$). As shown in Figure 5, FA activated significantly more voxel than correct target responses in all 4 ROIs (all $P < 0.05$, Bonferroni corrected for multiple comparisons). Furthermore, only rACC in the right hemisphere responded stronger to CR than to correct target responses ($t_{63} = 2.7$, $P = 0.05$, Bonferroni corrected for multiple

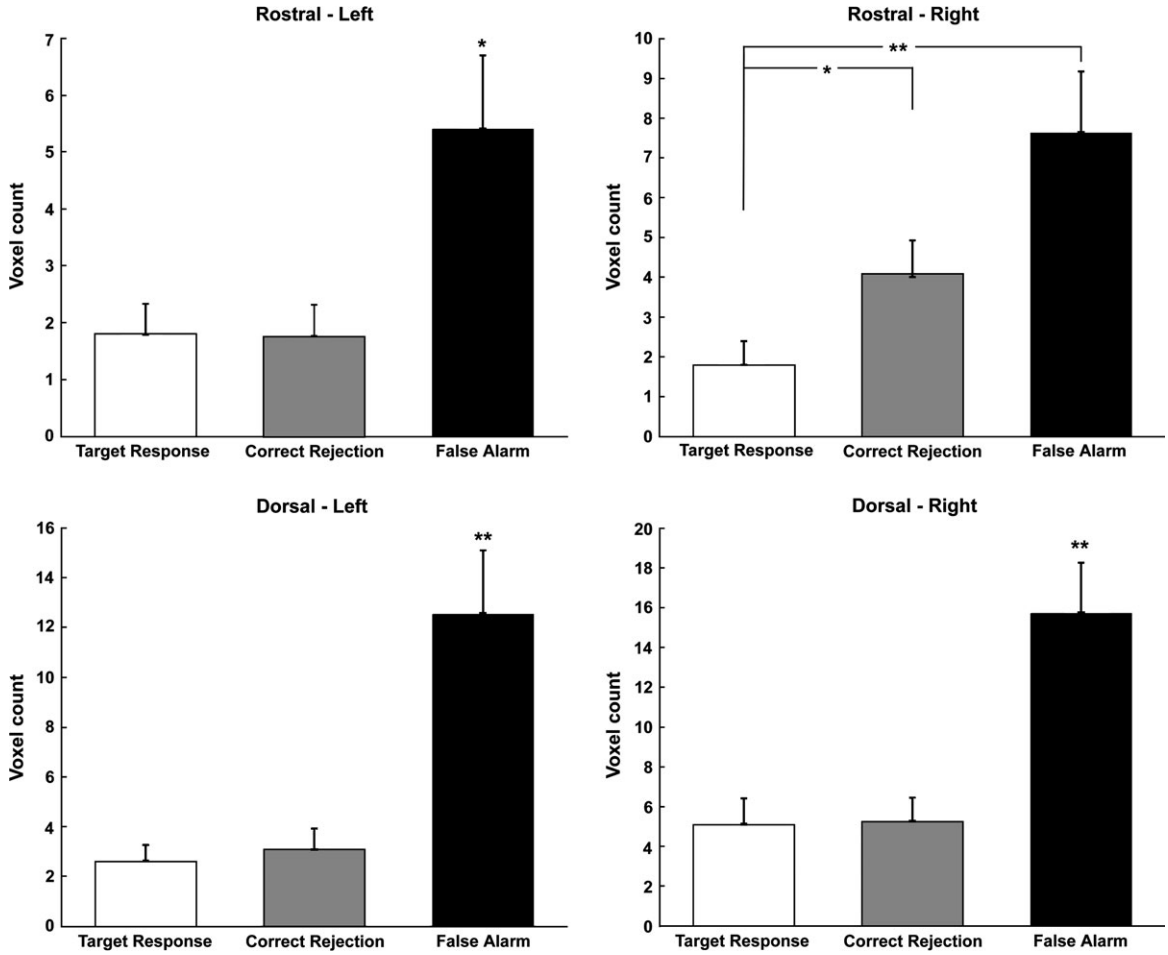

Figure 5. Mean number of activated voxels (single experiments) in dorsal and rostral as well as left and right ACCs. Whereas dACC as well as left rACC responded significantly stronger to FAs than to either correct target responses or CR, right dACC was activated by both CRs and FAs. $^{**}P \leq 0.01$, $^{*}P \leq 0.05$; Bonferroni corrected.

comparisons), whereas the number of voxels activated by FA did not differ from CR in this ROI ($t_{63} = 2.3$, $P = 0.1$). Such a pattern of activation would be expected if right rACC was to play a role in conflict monitoring, which is implicated by both CR and FA.

We obtained further evidence for a hemispheric specialization in ACC by calculating a "laterality index" for each subject from the number of activated voxels in right and left ACC (averaged across dorsal and rostral ROIs):

$$\text{laterality} = \frac{\text{Vox}_{\text{right}} - \text{Vox}_{\text{left}}}{\text{Vox}_{\text{right}} + \text{Vox}_{\text{left}}}$$

This index shows a strongly right-lateralized ACC response for CRs (0.73 ± 0.09), whereas FAs elicit a more bilateral response, though skewed to the right (0.27 ± 0.12).

Because the number of activated voxels only takes into account a very small fraction of the information that is available (and depends on the particular technique and cutoff used for thresholding), we additionally extracted and compared the normalized mean parameter estimates (beta values) of the fitted model for FA, CR, and correct target responses from the 4 ROIs (see Fig. 6). In accordance with the previous analysis, FA was associated with significantly stronger brain activation than correct button presses in all 4 ROIs (all $P < 0.01$, Bonferroni corrected for multiple comparisons). Furthermore, both left and right dACCs responded stronger to FA than to CR ($t_{63} = 5.1$, $P < 0.01$; $t_{63} = 4.6$, $P < 0.01$, respectively), whereas these comparisons failed to reach significance in rACC ($t_{63} = 2.1$, $P > 0.1$ and $t_{63} = 1.4$, $P > 0.1$, respectively). As before, right rACC responded significantly stronger to CR than to correct target responses ($t_{63} = 2.9$, $P < 0.05$), supporting a role for the region in conflict related processes.

Discussion

In this study, we used fMRI at high spatial resolution to uncover the functional microanatomy of human ACC during conflict monitoring and error processing. In line with previous studies, standard fMRI demonstrated a stronger ACC response for erroneous trials than for successful inhibitions. Based on these results, we imaged activated regions in MFC with higher spatial resolution and were able to obtain highly localized activation maps of neural foci both for conflict and error processing in the majority of subjects. Furthermore, these maps proved to be surprisingly reproducible. A multisubject analysis demonstrated bilateral error and right-lateralized conflict-associated processing in MFC as well as a cluster in right frontopolar cortex that responded significantly to Nogo trials. Subsequent ROI analysis largely agreed with the conclusions derived from high-resolution activation maps. Left rACC, as well as dACC, responded significantly to incorrect Nogo trials only and presumably play

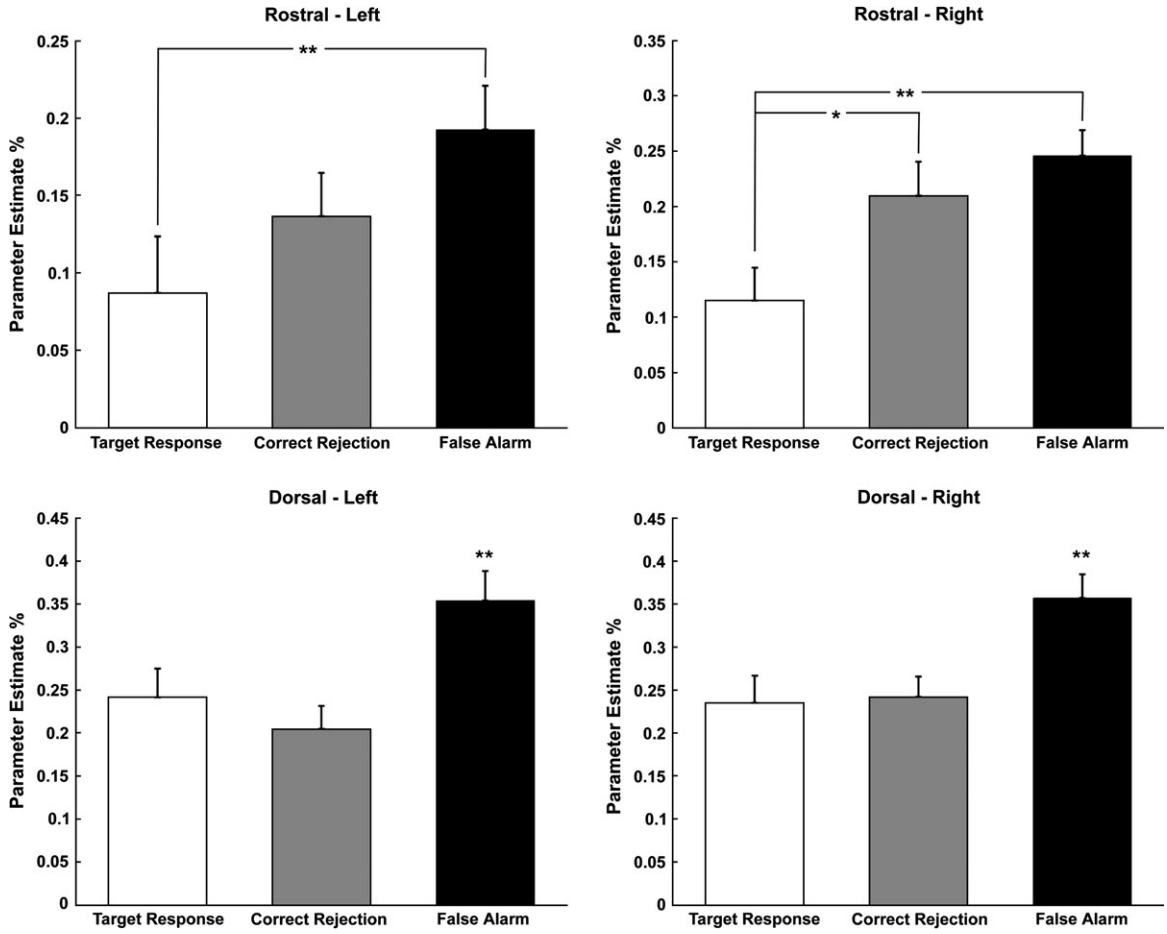

Figure 6. Mean parameter estimates of the fitted model in dorsal and rostral as well as left and right ACC. Whereas activation in dACC was associated with impulse errors, rACC in the right hemisphere responded significantly to errors as well as successful inhibitions. Left rACC responded significantly stronger to FAs than to target responses whereas responses to CRs did not differ from either FAs or target responses. $**P \leq 0.01$, $*P \leq 0.05$; Bonferroni corrected.

a role in error-related processes, such as error detection or evaluational aspects of error commission. Conversely, right rACC was activated both for successful and unsuccessful inhibition, albeit more strongly for the latter. This suggests that the region plays a role in monitoring and resolving cognitive conflict.

Although a number of previous GoNogo studies have reported conflict and error-related ACC activation (Konishi et al. 1998; Menon et al. 2001; Garavan et al. 2003), they remained inconclusive with respect to a differential involvement of the 2 hemispheres. Whereas lateralization was not mentioned in the majority of studies, some groups reported a specialization of either the left (Rubia et al. 2001) or the right hemisphere (Garavan et al. 1999) for conflict monitoring. In agreement with our results, Taylor et al. (2006) found that in a Flanker task, high conflict activation foci of individual subjects tended to cluster in the right MFC, whereas brain responses to errors were distributed more bilaterally. Stephan et al. (2003) showed, by analyzing effective connectivity, that ACC in the hemisphere that was occupied with the task at hand, also mediated the influence of cognitive control on the involved regions. Accordingly, for a visuospatial interference task that involved the right hemisphere, right ACC was also involved in monitoring for conflict, whereas left ACC mediated cognitive control when subjects processed verbal stimuli. These results seem to be at odds with the findings in our study because we used letter stimuli but nevertheless found conflict-related activation in the right ACC. It is, however, unclear to what extent subjects processed single letters verbally. Indeed, when we contrasted successful inhibition with FAs at standard resolution, the active cluster in inferior parietal cortex was close to the visuospatial activation reported by Stephan et al. (2003) yielding maximum voxel coordinates of 46, –76, 34 versus 54, –64, 42. This suggests that our subjects may have been relying more on configurational cues in solving the task than on verbal information about the letters. Further evidence for such a speculation derives from several subjects' introspective report that they did not verbalize the letters during the experiment.

Taken together, our results are in broad agreement with 2 previous studies that investigated the hemispheric lateralization of cognitive control in ACC. Using high-resolution fMRI, however, we were able to show for the first time directly that the right part of rACC mediated cognitive control in a letter-based GoNogo task, whereas left rACC as well as dACC were more concerned with error processing. It remains a question for future research whether dissociation between right and left ACC can be shown for tasks that are explicitly verbal or spatial (such as word or spatial GoNogo paradigms). Furthermore, it would be interesting to see if the opposite hemisphere always continues to process error-related information (as in our study).

Such a scenario would be in accordance with current models of conflict monitoring and error processing (Yeung et al. 2004). Thus, the ACC in the task-dominant hemisphere is implicated in cognitive control and monitors for conflict. Once conflict rises above a certain threshold, an error is assumed and the contralateral ACC is activated to initiate error-related processing. This interpretation would also explain why, in our study, right rACC was more strongly activated for errors than for CRs because errors simply are envisaged as situations of very high conflict.

Why did so many previous imaging studies detect no or inconsistent lateralization results in ACC? Considering the close proximity of both cortices as well as standard fMRI methodology, the failure to reliably identify lateralization is not very surprising. The average distance between left and right ACC, which are only separated by the interhemispheric fissure, is on the order of 1 cm. It can be shown that, with an image resolution of $3 \times 3 \times 3$ mm^3 and the use of substantial spatial smoothing (Scouten et al. 2006), such as a Gaussian kernel of 5 mm FWHM, focal neural activations in left and right ACCs may become at least partly indistinguishable. Inaccuracies introduced by imperfect spatial normalization (Hellier et al. 2003) as well as group averaging and the considerable variability of ACC anatomy (Paus et al. 1996; Huster et al. 2007) may have further contributed to the discrepancies in previous studies.

Although the primary aim of our study was to investigate the functional anatomy of ACC at high spatial resolution, we also detected a region in right frontopolar cortex that responded significantly to successful inhibitions as well as FAs and therefore presumably plays a role in conflict monitoring processes. Previously, Carlson et al. (1998) observed frontopolar activation when contrasting conditions of high and low memory load in a visuospatial *n*-back task. Furthermore, in a Stroop task, activation of right frontopolar brain areas was associated with the incongruent condition (Zysset et al. 2001). These experiments, together with results from the current study, provide support for the idea that lateral prefrontal cortex plays an important role in neural processes associated with cognitive conflict. Furthermore, the similar patterns of activation in right ACC and frontopolar cortex are in line with the conflict monitoring hypothesis of anterior cingulate function (Botvinick et al. 2001; Botvinick et al. 2004). In this model, ACC is thought to monitor for cognitive conflict and recruit other brain regions, such as lateral prefrontal cortex, which bring about behavioral readjustments to minimize subsequent conflict.

fMRI at an effective resolution (including postacquisition smoothing) comparable with that employed in the present study has previously been used solely to investigate the functional organization in subregions of the early visual system (Schneider et al. 2004; Schwarzlose et al. 2005; Grill-Spector et al. 2006). Here we demonstrate the feasibility of such an approach for brain regions involved in higher level processes, such as cognitive control. Improving the spatial resolution by a factor of 8 enabled us to explore the functional organization of ACC at a previously unaccomplished spatial scale and to reveal a dissociation between left and right ACC that has not been directly observed with standard techniques. Consequently, it may turn out fruitful to revisit a number of paradigms that have been reported to elicit ACC activation including pain stimulation (Jones et al. 1991; Talbot et al. 1991; Koyama et al. 2005) or emotional processing (Whalen et al. 1998; Bush et al. 2000). We predict that at high resolution a number of regional specializations will become apparent for stimuli and tasks that have so far been mapped to overlapping locations. Furthermore, given the high functional and anatomical variability in ACC, we would recommend extensive analysis of single-subject data in addition to traditional group approaches.

Importantly, high-resolution fMRI should be considered as a complementary technique to standard neuroimaging rather than as a replacement. Whereas standard approaches provide the benefits of whole-brain coverage in a reasonable time frame, good signal-to-noise ratio, and also offer the opportunity to estimate functional connectivity, high-resolution fMRI is limited in these respects. Indeed, the technique may be envisaged as "zooming into" a region that was previously identified as active by established imaging strategies. Although this approach has been used routinely to study early visual processing, we present the first successful attempt, to our knowledge, of mapping a higher level brain area in this way. We believe that the "zooming in" fMRI strategy will provide a powerful new tool for cognitive neuroscientists. It may help bridging the gap between neuroimaging and electrode recording and thereby contribute to our understanding of the neural basis of cognition.

In summary, our findings demonstrate a functional specialization in ACC: whereas the right rACC is involved in conflict monitoring, its left part as well as dACC activated solely for error-related processes. More generally, our study illustrates the usefulness of high-resolution fMRI to identify functional specializations in higher level, cognitively driven brain areas.

Supplementary Material

Supplementary material can be found at http://www.cercor.oxfordjournals.org/.

Notes

We would like to thank Klaus-Dietmar Merboldt and Dirk Voit for their help with the imaging protocols as well as Renate Schweizer for her comments on the manuscript. Parts of the work were presented at the 36th Annual Meeting of the Society for Neuroscience (Atlanta, GA) in October 2006. *Conflict of Interest*: None declared.

Address correspondence to email: hluetck@gwdg.de.

References

Beckmann CF, Jenkinson M, Smith SM. 2003. General multilevel linear modeling for group analysis in FMRI. Neuroimage. 20:1052–1063.

Botvinick M, Nystrom LE, Fissell K, Carter CS, Cohen JD. 1999. Conflict monitoring versus selection-for-action in anterior cingulate cortex. Nature. 402:179–181.

Botvinick MM, Braver TS, Barch DM, Carter CS, Cohen JD. 2001. Conflict monitoring and cognitive control. Psychol Rev. 108:624–652.

Botvinick MM, Cohen JD, Carter CS. 2004. Conflict monitoring and anterior cingulate cortex: an update. Trends Cogn Sci. 8:539–546.

Bush G, Luu P, Posner MI. 2000. Cognitive and emotional influences in anterior cingulate cortex. Trends Cogn Sci. 4:215–222.

Carlson S, Martinkauppi S, Rama P, Salli E, Korvenoja A, Aronen HJ. 1998. Distribution of cortical activation during visuospatial n-back tasks as revealed by functional magnetic resonance imaging. Cereb Cortex. 8:743–752.

Carter CS, Braver TS, Barch DM, Botvinick MM, Noll D, Cohen JD. 1998. Anterior cingulate cortex, error detection, and the online monitoring of performance. Science. 280:747–749.

Devinsky O, Morrell MJ, Vogt BA. 1995. Contributions of anterior cingulate cortex to behaviour. Brain. 118(Pt 1):279–306.

Falkenstein M, Hohnsbein J, Hoormann J, Blanke L. 1991. Effects of crossmodal divided attention on late ERP components. 2. Error processing in choice reaction tasks. Electroencephalogr Clin Neurophysiol. 78:447–455.

Garavan H, Ross TJ, Kaufman J, Stein EA. 2003. A midline dissociation between error-processing and response-conflict monitoring. Neuroimage. 20:1132–1139.
Garavan H, Ross TJ, Stein EA. 1999. Right hemispheric dominance of inhibitory control: an event-related functional MRI study. Proc Natl Acad Sci USA. 96:8301–8306.
Gehring WJ, Goss B, Coles MGH, Meyer DE, Donchin E. 1993. A Neural system for error-detection and compensation. Psychol Sci. 4:385–390.
Genovese CR, Lazar NA, Nichols T. 2002. Thresholding of statistical maps in functional neuroimaging using the false discovery rate. Neuroimage. 15:870–878.
Grill-Spector K, Sayres R, Ress D. 2006. High-resolution imaging reveals highly selective nonface clusters in the fusiform face area. Nat Neurosci. 9:1177–1185.
Hellier P, Barillot C, Corouge I, Gibaud B, Le Goualher G, Collins DL, Evans A, Malandaln G, Ayache N, Christensen GE, et al. 2003. Retrospective evaluation of intersubject brain registration. IEEE Trans Med Imaging. 22:1120–1130.
Huster RJ, Westerhausen R, Kreuder F, Schweiger E, Wittling W. 2007. Morphologic asymmetry of the human anterior cingulate cortex. Neuroimage. 34:888–895.
Jenkinson M, Bannister P, Brady M, Smith S. 2002. Improved optimization for the robust and accurate linear registration and motion correction of brain images. Neuroimage. 17:825–841.
Jenkinson M, Smith S. 2001. A global optimisation method for robust affine registration of brain images. Med Image Anal. 5:143–156.
Jones AKP, Brown WD, Friston KJ, Qi LY, Frackowiak RSJ. 1991. Cortical and subcortical localization of response to pain in man using positron emission tomography. Proc R Soc Lond B Biol Sci. 244:39–44.
Kiehl KA, Liddle PF, Hopfinger JB. 2000. Error processing and the rostral anterior cingulate: an event-related fMRI study. Psychophysiology. 37:216–223.
Konishi S, Nakajima K, Uchida I, Sekihara K, Miyashita Y. 1998. No-go dominant brain activity in human inferior prefrontal cortex revealed by functional magnetic resonance imaging. Eur J Neurosci. 10: 1209–1213.
Koyama T, McHaffie JG, Laurienti PJ, Coghill RC. 2005. The subjective experience of pain: where expectations become reality. Proc Natl Acad Sci USA. 102:12950–12955.
Menon V, Adleman NE, White CD, Glover GH, Reiss AL. 2001. Error-related brain activation during a Go/NoGo response inhibition task. Hum Brain Mapp. 12:131–143.
Paus T, Tomaiuolo F, Otaky N, MacDonald D, Petrides M, Atlas J, Morris R, Evans AC. 1996. Human cingulate and paracingulate sulci: pattern, variability, asymmetry, and probabilistic map. Cereb Cortex. 6: 207–214.
Polli FE, Barton JJ, Cain MS, Thakkar KN, Rauch SL, Manoach DS. 2005. Rostral and dorsal anterior cingulate cortex make dissociable contributions during antisaccade error commission. Proc Natl Acad Sci USA. 102:15700–15705.
Ridderinkhof KR, Ullsperger M, Crone EA, Nieuwenhuis S. 2004. The role of the medial frontal cortex in cognitive control. Science. 306: 443–447.
Ridderinkhof KR, van den Wildenberg WPM, Segalowitz SJ, Carter CS. 2004. Neurocognitive mechanisms of cognitive control: the role of prefrontal cortex in action selection, response inhibition, performance monitoring, and reward-based learning. Brain Cogn. 56: 129–140.
Rubia K, Russell T, Overmeyer S, Brammer MJ, Bullmore ET, Sharma T, Simmons A, Williams SC, Giampietro V, Andrew CM, et al. 2001. Mapping motor inhibition: conjunctive brain activations across different versions of go/no-go and stop tasks. Neuroimage. 13: 250–261.
Schneider KA, Richter MC, Kastner S. 2004. Retinotopic organization and functional subdivisions of the human lateral geniculate nucleus: a high-resolution functional magnetic resonance imaging study. J Neurosci. 24:8975–8985.
Schwarzlose RF, Baker CI, Kanwisher N. 2005. Separate face and body selectivity on the fusiform gyrus. J Neurosci. 25:11055–11059.
Scouten A, Papademetris X, Constable RT. 2006. Spatial resolution, signal-to-noise ratio, and smoothing in multi-subject functional MRI studies. Neuroimage. 30:787–793.
Smith SM. 2002. Fast robust automated brain extraction. Hum Brain Mapp. 17:143–155.
Smith SM, Brady JM. 1997. Susan—a new approach to low level image processing. Int J Comput Vis. 23:45–78.
Stephan KE, Marshall JC, Friston KJ, Rowe JB, Ritzl A, Zilles K, Fink GR. 2003. Lateralized cognitive processes and lateralized task control in the human brain. Science. 301:384–386.
Talbot JD, Marrett S, Evans AC, Meyer E, Bushnell MC, Duncan GH. 1991. Multiple representations of pain in human cerebral-cortex. Science. 251:1355–1358.
Taylor SF, Martis B, Fitzgerald KD, Welsh RC, Abelson JL, Liberzon I, Himle JA, Gehring WJ. 2006. Medial frontal cortex activity and loss-related responses to errors. J Neurosci. 26:4063–4070.
Ullsperger M, von Cramon DY. 2004. Neuroimaging of performance monitoring: error detection and beyond. Cortex. 40:593–604.
Whalen PJ, Bush G, McNally RJ, Wilhelm S, McInerney SC, Jenike MA, Rauch SL. 1998. The emotional counting stroop paradigm: a functional magnetic resonance imaging probe of the anterior cingulate affective division. Biol Psychiatry. 44:1219–1228.
Woolrich MW, Behrens TEJ, Beckmann CF, Jenkinson M, Smith SM. 2004. Multilevel linear modelling for FMRI group analysis using Bayesian inference. Neuroimage. 21:1732–1747.
Woolrich MW, Ripley BD, Brady M, Smith SM. 2001. Temporal autocorrelation in univariate linear modeling of FMRI data. Neuroimage. 14:1370–1386.
Worsley KJ, Evans AC, Marrett S, Neelin P. 1992. A three-dimensional statistical analysis for CBF activation studies in human brain. J Cereb Blood Flow Metab. 12:900–918.
Yeung N, Botvinick MM, Cohen JD. 2004. The neural basis of error detection: conflict monitoring and the error-related negativity. Psychol Rev. 111:931–959.
Zysset S, Muller K, Lohmann G, von Cramon DY. 2001. Color-word matching stroop task: separating interference and response conflict. Neuroimage. 13:29–36.